RESEARCH ARTICLE

Application of Design of Experiment in the Optimization of Apixaban-Loaded Solid Lipid Nanoparticles: *In Vitro* and *In Vivo* Evaluation

Safaa E. Ramadan[1] [ORCID] · **Sanaa A. El-Gizawy[1]** · **Mohamed A. Osman[1]** · **Mona F. Arafa[1]**

Abstract

Solid lipid nanoparticles (SLnPs) are usually utilized as lipid-based formulations for enhancing oral bioavailability of BCS class IV drugs. Accordingly, the objective of this work was to investigate the effect of formulation and processing variables on the properties of the developed SLnPs for oral delivery of apixaban. Randomized full factorial design (2^4) was employed for optimization of SLnPs. With two levels for each independent variable, four factors comprising both formulations and processing factors were chosen: the GMS content (A), the Tween 80 content (B), the homogenization time (C), and the content of poloxamer 188 used (D). The modified hot homogenization and sonication method was employed in the formulation of solid lipid nanoparticles loaded with apixaban (APX-SLnPs). The size of APX-SLnPs formulations was measured to lie between 116.7 and 1866 nm, polydispersity index ranged from 0.385 to 1, and zeta potential was discovered to be in the range of -12.6 to -38.6 mV. The entrapping efficiency of APX-SLnPs formulations was found to be in the range of 22.8 to 96.7%. The optimized formulation was evaluated *in vivo* after oral administration to rats. Oral administration of APX-SLnPs resulted in significant prolongation in bleeding time compared with both positive and negative control. This indicates the ability of this system to enhance drug therapeutic effect either by increasing intestinal absorption or trans-lymphatic transport. So, this study highlighted the capability of SLnPs to boost the pharmacological effect of apixaban.

Keywords apixaban · bleeding time · factorial design · poloxamer · solid lipid nanoparticles

Introduction

Large number of pharmacologically active drug candidates are categorized as class IV drugs according to the biopharmaceutical categorization system (BCS). Unfortunately, this class of drugs has certain obstacles which include poor aqueous solubility and limited permeability. In addition, most of these drugs are P-glycoprotein efflux transporter substrate and substrate for the metabolizing enzyme CYP3A4 which limits their systemic absorption and therapeutic potential [1]. These characteristics are challenging for pharmaceutical formulators to develop effective oral delivery systems. Hence, several formulation approaches were investigated as fruitful BCS class IV drug delivery systems. These approaches include polymer-based nanocarriers [2, 3], crystalline structure modification via nano-crystallization and co-crystal formation [4, 5], liquisolid technique [6], self-emulsification and self-microemulsification [7], and systems based on lipids [8].

Solid lipid nanoparticles (SLnPs) are one of the utilized lipid-based formulations for making the BCS class IV drugs orally bioavailable. They serve as an alternative particulate nanocarrier system to polymeric nanoparticles, liposomes, and emulsions (o/w) [9–13]. SLnPs aqueous dispersions comprise lipids (solid at body and room temperatures) that are stabilized using an appropriate surfactant. SLnPs represent an advantageous approach based on their exceptional properties which include the ability to encapsulate

✉ Safaa E. Ramadan
safaa.eid@pharm.tanta.edu.eg

Sanaa A. El-Gizawy
Sanaa.elgizawi@pharm.tanta.edu.eg

Mohamed A. Osman
Mohamed.ibrahim5@pharm.tanta.edu.eg

Mona F. Arafa
mona.arafa@pharm.tanta.edu.eg

[1] Department of Pharmaceutical Technology, Faculty of Pharmacy, Tanta University, Tanta, Egypt

hydrophobic and hydrophilic active moieties, the small size, and high drug loading capacity which facilitate lymphatic uptake escaping first-pass metabolism [14]. In addition, they are utilized to improve permeability and palatability and achieve controlled or sustained drug release [15–17]. Besides, SLnPs reported high physical stability and acceptable biodegradability.

Many methods can be employed for the production of SLnPs. However, homogenization followed by ultrasonication is the most frequently employed method [18]. It is more valuable than the other techniques due to short making time, the availability of industrial homogenization lines, the adequacy of homogenization tools by different regulatory authorities, ease of scaling up, and the feasibility of avoiding the negative impact of organic solvents in the production process [19, 20].

Apixaban (APX) is a model of class IV drugs. It is a potent anticoagulant that when administered orally inhibits the coagulation factor Xa selectively and directly. So, apixaban is frequently used as a preventive treatment for the avoidance of venous thromboembolism [21]. FDA-approved apixaban in preventing embolism in non-valvular atrial fibrillation patients and for avoiding stroke. Recently, it was investigated in several research works for the prevention of thrombosis in COVID 19 patients [22]. Unfortunately, the water solubility of APX is poor (40–50 µg/mL) [23], and the oral bioavailability after administration of a unit dose (10 mg) is limited (about 50%). Apixaban's observed low bioavailability was attributed to the drug's insufficient absorption in the digestive system in addition to the effect of hepatic and intestinal first-pass metabolism [23]. The formulation of APX as SLnPs may improve the oral bioavailability of the drug and retain it in systemic circulation for a sustained period.

Accordingly, the principal goal of this research was to produce, optimize, and characterize APX-SLnPs using a full factorial design. The aim was to investigate the impact of both processing and formulation variables on the properties of the developed solid lipid nanoparticles. Full factorial design was selected as it is the pharmaceutical industry's most practical design that is very beneficial for preliminary studies and initial optimization [24, 25]. The developed APX-SLnPs were assessed regarding particle size, PDI, entrapment efficiency, zeta potential, and apixaban release kinetics. The study was extended for *in vivo* assessment of the optimized solid lipid nanoparticles encapsulating apixaban using bleeding model. The results of this *in vivo* study can provide a direct reflection of the therapeutic effect of apixaban from solid lipid nanoparticles relative to that of the aqueous suspension of apixaban. The *in vivo* study was preferred over the ex vivo study as it takes into its account the role of trans lymphatic absorption of the drug which cannot be reflected in the results of ex vivo permeation studies.

Materials and Methods

Materials

Apixaban (APX) was obtained as a gift from ATCO Pharma for pharmaceutical industries, Egypt. Glycerol mono stearate (GMS) which is a solid lipid was obtained from El Qahera for Pharmaceutical & Chemical Industries, Egypt. The surfactants that were utilized in this work included Tween 80 from El-Nasr Pharmaceutical Chemical Co., Egypt, Poloxamer 188 (Pluronic F68) from Amoun Pharmaceutical Co., Egypt, and Poloxamer 407 (Pluronic F127) from Sigma for Pharmaceutical Industries. Ketamine had been received as a gift from EIPICO for Pharmaceutical Industries. Acetonitrile (HPLC grade) was purchased from SDFCL (S D Fine-Chem Limited, Mumbai, India). Disodium hydrogen phosphate was acquired from Lanxess AG, India.

Experimental Design and Statistical Analysis

To attain the optimum physicochemical characteristics of apixaban solid lipid nanoparticles (APX-SLnPs), 2^4 randomized full factorial design was employed. In this study, with two levels for each independent variable, four factors were chosen: the GMS content (A) at two levels (200 mg and 250 mg), the Tween 80 content (B) at two levels (50 mg and 100 mg), the homogenization time (C) at two levels (3 min and 6 min), and content of poloxamer 188 used (D) at two levels (mixture of poloxamer 188 and poloxamer 407 each of 150 mg and poloxamer 188 (300 mg)). Table I displays the low and high levels for each factor.

Table I Coded Values of 2^4 Full Factorial Design for Formulation of APX-SLnPs

Independent variables	Levels	
	Low	High
A (GMS content (mg))	200	250
B (Tween 80 content (mg))	50	100
C (Homogenization time (min))	3	6
D (Content of poloxamer188 (mg))	150	300
Coded values	−1	+1

The low level in the content of poloxamer is a mixture of poloxamer 188 and poloxamer 407; each of 150 mg and high level represents poloxamer 188 (300 mg)

GMS, glycerol mono stearate; *APX-SLnPs*, solid lipid nanoparticles loaded with apixaban

Preparation of APX-SLnPs

The modified hot homogenization and sonication method was employed in the preparation of APX-SLnPs. This approach was already used in numerous research projects as an efficient method for the preparation of this nano system [26–28]. Briefly, a mixture of apixaban, GMS, and Tween 80 was dissolved in ethanol (10 mL). This organic solvent mixture was allowed to evaporate totally at 70°C leaving drug-embedded lipid layer onto the beaker. This layer was heated at 10°C over the lipid melting point to allow its melting. The heated aqueous phase (70°C) comprising poloxamer dissolved in 40 mL of distilled water was added to the melted lipid after that they were homogenized using a polytron homogenizer (PT-MR 3100 KINEMATICA AG Littau -Switzerland) at 14,000 rpm for either 3 or 6 min. This was followed by a 10-min sonication. Different APX-SLnPs formulations were prepared with their compositions being shown in Table II.

MINITAB statistical software (Minitab release 18) was manipulated to statistically analyze the derived parameters. ANOVA statistical analysis was used in this, along with the creation of model equations and the construction of Pareto charts and contour plots for each response. Particle size (minimize), entrapment efficiency (maximize), % apixaban released (minimize), and T_{50} (maximize) were chosen as the critical quality parameters. The factorial design was analyzed statistically using multiple regression analysis. Equation (1) describes a statistical model that was employed to assess the response.

$$Y = b0 + b1A + b2B + b3C + b4D + b12AB + b13AC$$
$$+ b14AD + b23BC + b24BD + b34CD + b123ABC$$
$$+ b124ABD + b234BCD + b1234ABCD$$

$$(1)$$

The dependent variable is Y, and the assessed coefficient of factor I is bi. The 16 runs' arithmetic mean response is represented by b0. The main effects (A, B, C, and D) show what happens when one factor is changed from a low level to a higher level on average. The term interaction demonstrates how the response alters once two factors are concurrently modified.

In Vitro Characterization of APX-SLnPs

Particle Size, Polydispersity Index, and Zeta Potential

The particle size, poly dispersibility index, and zeta potential of the prepared APX-SLnPs were measured using Nano Zetasizer series (Nano-ZS, Malvern Instruments, UK). The sample manipulation included dilution 15 times with distilled water before loading into capillary cells for

Table II Full Factorial Design with Coded and Actual Values Used for the Optimization of APX-SLnPs Formulations

Formula	Coded values				Actual value			
	A	B	C	D	GMS content (mg)	Tween 80 content (mg)	Homogeniza-tion time (min)	Content of poloxamer 188 (mg)*
					(A)	(B)	(C)	(D)
F1	-	-	-	-	200	50	3	150
F2	+	-	-	-	250	50	3	150
F3	-	+	-	-	200	100	3	150
F4	+	+	-	-	250	100	3	150
F5	-	-	+	-	200	50	6	150
F6	+	-	+	-	250	50	6	150
F7	-	+	+	-	200	100	6	150
F8	+	+	+	-	250	100	6	150
F9	-	-	-	+	200	50	3	300
F10	+	-	-	+	250	50	3	300
F11	-	+	-	+	200	100	3	300
F12	+	+	-	+	250	100	3	300
F13	-	-	+	+	200	50	6	300
F14	+	-	+	+	250	50	6	300
F15	-	+	+	+	200	100	6	300
F 16	+	+	+	+	250	100	6	300

*The low level in the content of poloxamer is mixture of poloxamer 188 and poloxamer 407 each of 150 mg, and high level represents poloxamer 188 (300 mg)

APX-SLnPs, solid lipid nanoparticles loaded with apixaban; *GMS*, glycerol mono stearate

assessing the size and zeta potential. Each measurement was repeated three times at 25°C.

Determination of Percentage Entrapment Efficiency and Apixaban Loading

Percent entrapment efficiency (% EE) was estimated by dialysis approach. This method was reported previously [29, 30]. The dialysis tubing cellulose membrane (cellulose tube with 14,000 Daltons cut off, Sigma-Aldrich, St. Louis, MO) was left in distilled water for the entire day till complete hydration to guarantee fixed pore diameter. APX-SLnPs dispersion (2 ml) was packed within the dialysis tube (5.5 cm) that was securely tied from both ends with threads. The dialysis bag was freely immersed in a glass beaker containing 100 ml disodium hydrogen phosphate solution (DSP) (pH 6.8) at ambient temperature. After 6 h, samples were withdrawn and analyzed for free apixaban concentration by the developed HPLC method. Deducing the amount of the free unentrapped apixaban from the entire drug present in the sample provides the amount of the entrapped apixaban. The following equations were utilized for computing the % EE (Eq. 2) and % drug loading (Eq. 3) of the prepared APX-SLnPs:

$$EE\ (\%) = \frac{\text{The amount of entrapped drug}}{\text{The total amount of drug}} \times 100 \qquad (2)$$

$$\text{Drug loading}\ (\%) = \frac{\text{The weight of drug in nanoparticles}}{\text{The total weight of nanoparticles}} \times 100 \quad (3)$$

In Vitro Apixaban Release Studies

The study of *in vitro* apixaban release was conducted to determine the release rate and kinetics of apixaban from the prepared SLnPs. The release rate from drug suspension was determined and taken as a positive control. Franz cells (vertical glass diffusion cells) with a receptor volume of 14.5 ml and a surface area of 2.27 cm^2 for diffusion were used for this study. This method was frequently employed in several research works [26, 31, 32]. Semipermeable cellulose membrane (MW cutoff 14,000) was immersed in distilled water overnight after being cut into pieces of appropriate size. After complete hydration, the membrane was positioned between the diffusion cells' donor and receptor parts. The receptor was filled with DSP that was chosen as the release media to preserve sink conditions during the experiment. The release study was performed at 37 ± 1°C to simulate the *in vivo* temperature. The tested formulation (2 ml) was piled into the donor, and samples (5 ml) from the receptor compartment were taken at definite time intervals and were analyzed for drug concentration by HPLC method. After sample withdrawal, fresh media was added to retain constant receptor compartment volume. Each experiment was carried out three times.

Apixaban Release Kinetic Studies

The release data of APX from the developed SLnPs was analyzed using DDsolver software. The obtained data were fitted to several kinetic models which involve zero-order model, first-order model, and Higuchi model to explore the release mechanism, and the cumulative percentage of drug release was charted *versus* time.

Fourier-Transform Infrared Spectroscopy (FTIR)

The FTIR spectra of apixaban, glyceryl monostearate, poloxamer 188, the optimized formula, and the physical mixture were collected using an FTIR spectrophotometer (FTIR SPECTROMETER 4100 JASCO-JAPAN). The optimized formulation was centrifuged using SIGMA 3-30 K (SIGMA Laborzentrifugen, Osterode am Harz, Germany) for 2 h at a centrifugation speed of 25,000 rpm, and the obtained precipitate was employed in spectral analysis. Before being compressed into flat discs using a hydraulic press, the test powders were combined with a spectroscopic grade of KBr. The discs were scanned from 4000 to 400 cm^{-1}. JASCO's exclusive Spectra Manager™ II cross-platform software was used for data analysis. A DLaTGS detector supports the spectrophotometer.

Differential Scanning Calorimetry (DSC)

Thermal analysis was performed for APX powder, GMS, Pluronic F68, the physically mixed solid ingredients (at a similar ratio as in the formula), and the centrifuged form of the optimized SLnPs. The differential scanning calorimeter that was employed for thermal analysis was the Discovery DSC 25-TA instrument (Newcastle, DE, USA). The accurately weighed amount of each sample was filled into a zero alumina pan before being crimped with a pan lid and loaded into the equipment. The analysis covered a range of 25–400°C with a 10°C/min heating rate. The recorded data was manipulated using TRIOS software.

Transmission Electron Microscopy (TEM)

Utilizing a transmission electron microscope (JEM-1400 Plus, Jeol, Tokyo, Japan), the optimized APX-SLnPs' surface morphology and shape were determined. A drop of the optimized SLnPs was put on a carbon-coated grid. After being adsorbed by the grid, the sample was dyed

with uranyl acetate for 5 min. After that, the sample was stained with lead citrate for 2 min. The dyed grid was observed under TEM, and appropriate magnification was selected to take pictures.

High-Pressure Liquid Chromatography (HPLC)

Using an HPLC system provided by Agilent Technologies (1260 Infinity, DE, Germany), apixaban was quantified in the experimental samples. This system is equipped with a 1260-UV detector and TCC 1260 automatic sampling system for sample injection. Drug separation was achieved on the C18 column (150 mm × 4.6 mm) with 5 µm particles being packed in (Inter-sil®, GL Sciences Inc., Tokyo, Japan). The mobile phase was a blend of filtered distilled water and acetonitrile at a ratio of 60:40 which was pumped at a rate of 1 ml/min. Sample with a volume of 30 microliter was injected, and the effluent was detected at a wavelength of 280 nm. The system was fully computerized and controlled via the software (Agilent Open-LAB ChemStation). This software was used to modify the experimental setup and carry out the data analysis. The method of assay was validated with respect to linearity, accuracy, precision, and limit of detection and quantification (LOD and LOQ).

Investigation of Anticoagulant Effect by Bleeding Model

The anticoagulant effect of apixaban formulated in SLnPs was studied utilizing bleeding model. This model was previously employed in several research works [33, 34]. The study employed 18 male albino rats with an average weight of 200 g. The College of Pharmacy at the University of Tanta's Ethical Committee approved the methodology which involved rats' manipulation and duration of the study with an approval number of PT 00100. Three groups of six rats each were created out of the animals. Group I was kept as the naïve group (negative control) which did not receive pure drug nor drug-loaded SLnPs. Group II was treated orally with drug suspension (positive control) with a dose of 0.89 mg/kg. Group III was treated orally with apixaban-loaded SLnPs (test group) with a dose of 0.89 mg/kg.

After 3 h of drug administration, each rat was anesthetized via injection of ketamine (intraperitoneal) with a dose of 100 mg/kg. After being anesthetized, the rat was kept in a prone position on a platform. The tail of the rat was put horizontally on the table, and 5 mm from the tip of the tail was cut triggering bleeding. The blood was collected with no. 4 filter paper at different time intervals (seconds) till ceases to bleed and no blood was detected on the filter paper.

The time interval passed from the transection of the tail till the complete ceasing of bleeding was taken as bleeding time.

Results and Discussion

Particle Size and Zeta Potential

The mean particle size, polydispersity index, and zeta potential for APX-SLnPs are presented in Table III. The size of APX-SLnPs formulations was found to be ranged from 116.7 to 1866 nm. The polydispersity index laid in the range from 0.385 to 1 and the zeta potential was recorded to be between -12.6 and -38.6 mV.

The anticipated regression equation for the size of the particles is as follows:

$$\begin{aligned} size = & 518.47 + 145.19A + 54.64B - 157.00C \\ & + 175.53AB + 84.03AD + 133.23BD \\ & - 141.19CD - 41.79ABC - 156.72BCD \\ & - 144.59ACD - 81.17ABCD \end{aligned} \quad (4)$$

$R^2 =$ value was 0.988 and when ANOVA was used, the effects of all the investigated factors and interactions were significant statistically ($p < 0.05$) except for factor D (p value $= 0.561$) and interactions AC (p value $= 0.134$), BC (p value $= 0.218$), and ABD (p value $= 0.595$).

Conferring to Eq. (4), the most efficient factor in decreasing the particle size of APX- SLnPs formulation

Table III Average Particle Size, Polydispersity Index (PDI), and Zeta Potential for the APX-SLnPs formulations

Formula	Particle size (nm)	PDI	Zeta potential (mV)
F1	957 ± 71.79	0.843 ± 0.27	-24.5 ± 0.38
F2	551.6 ± 79.99	0.98 ± 0.3	-38.6 ± 0.6
F3	243.8 ± 34.79	0.576 ± 0.17	-18.5 ± 0.56
F4	365.2 ± 8.25	0.385 ± 0.007	-18.6 ± 0.46
F5	447.2 ± 46.58	0.518 ± 0.06	-13.4 ± 0.59
F6	412.9 ± 13.48	0.996 ± 0.006	-20.5 ± 0.31
F7	161.76 ± 5.4	0.416 ± 0.22	$-14.6 \pm .057$
F8	969.3 ± 65.04	0.69 ± 0.04	-19.6 ± 1.25
F9	285.7 ± 17.46	0.686 ± 0.04	-33.1 ± 0.52
F10	549.9 ± 58.94	1 ± 0	-23.6 ± 0.37
F11	487.3 ± 19.01	1 ± 0	-27.3 ± 0.42
F12	1866 ± 144.4	0.925 ± 0.13	-31.2 ± 0.49
F13	189.2 ± 0.75	0.425 ± 0.01	-17 ± 1.6
F14	219.5 ± 12.86	0.499 ± 0.05	-22.5 ± 0.35
F15	116.7 ± 3.05	0.527 ± 0.09	-12.6 ± 0.79
F16	375.1 ± 46.79	0.8 ± 0.12	-31.4 ± 3.1

PDI, polydispersity index; *APX-SLnPs*, solid lipid nanoparticles loaded with apixaban

was − AB (interaction between − A (200 mg GMS) and + B (100 mg Tween 80)), followed by + C homogenization time (6 min) and + BCD (interaction between + B Tween 80 (100 mg), + C homogenization time (6 min), and + D 300 mg of poloxamer 188).

The interaction between the lowest amount of lipid and the highest amount of Tween 80 was the most effective factor resulting in nano systems with smaller particle size.

In general, the high percentage of monoglycerides (the primary component of GMS) provides surface tension activity, which facilitates emulsification and enhances the surfactant film surrounding the nanoparticles, preventing particle aggregation and crystal growth [35]. Increasing the quantity of GMS increased the particle size. The propensity of lipid to coalesce at elevated lipid concentrations can be used to explain why the size of the particle increased as the GMS concentration was raised. Stake's law states that the variation in density between the interior and external phases can account for this behavior. Additionally, according to Schubert *et al.*, a rise in the particle size of SLnPs is caused by a decrease in the rate of solute molecule diffusion in the outer phase because of an increase in the viscosity of the lipid-solvent phase [36]. So, decreasing the amount of lipids leads to a reduction in particle size. In addition, at higher surfactant concentrations, there will be a decrease in the interfacial tension and gaps between particles that prevent or avoid the aggregation between particles and reduces the particle size [37].

The second effective factor is + C (homogenization time (6 min)) as the SLnPs particle size decreases with increasing the time of homogenization cycle. This was reported in literature [38].

The third effective factor is + BCD which is the interaction between higher levels of Tween 80, homogenization time 6 min, and 300 mg of poloxamer 188. The effect of higher levels of Tween 80 and homogenization time was discussed previously. The interaction between them and the high level of factor D may be explained by the higher HLB value for poloxamer 188 (HLB = 29) compared with the HLB value of the poloxamer mixture (HLB = 25.5). This significantly affects the stability of the SN dispersion and consequently the nano systems. Many literatures considered the particle size as the most critical factor in evaluating the efficacy of the developed SLnPs. It was reported that the smaller the particle size, the more efficient will be the nano system. This can be accredited to its ability to adhere to the biological membrane, increasing the residence time and hence the oral bioavailability [39]. Accordingly, F15 was selected as the optimized formula with respect to particle size.

Table IV The Percentage Entrapment Efficiency (EE) and % Drug Loading for All APX-SLnPs Formulations

Formula	EE %	Drug loading %
F1	80.1 ± 2.9	0.72 ± 0.03
F2	85.2 ± 1.8	0.7 ± 0.02
F3	32.3 ± 1.8	0.27 ± 0.03
F4	29.8 ± 0.28	0.23 ± 0.002
F5	38 ± 0.9	0.34 ± 0.02
F6	96.7 ± 1.4	0.8 ± 0.01
F7	36.1 ± 0.37	0.3 ± 0.02
F8	22.8 ± 1.4	0.19 ± 0.01
F9	66.8 ± 2	0.6 ± 0.02
F10	68.2 ± 1.4	0.56 ± 0.01
F11	82.5 ± 1.3	0.68 ± 0.01
F12	87.8 ± 2.9	0.67 ± 0.03
F13	37.2 ± 0.29	0.34 ± 0.002
F14	32.8 ± 1.09	0.27 ± 0.009
F15	27.2 ± 0.84	0.23 ± 0.006
F16	86.2 ± 8.1	0.66 ± 0.06

EE, entrapment efficiency; *APX-SLnPs*, solid lipid nanoparticles loaded with apixaban

Entrapment Efficiency

The trapping efficiency of APX-SLnPs ranged from 22.8 to 96.7%. The % apixaban loading was between 0.19 and 0.8%. The trapping efficiency and drug loading data are informed in Table IV.

The deduced regression equation for entrapping efficiency (EE %) is as follows:

$$EE = 56.862 + 6.834A - 6.257B - 9.742C + 4.246D - 0.769AB$$
$$+ 5.663AC + 0.818AD + 2.209BC + 16.104BD$$
$$- 5.505CD + 9.178ABD - 1.205BCD + 7.749ABCD$$

$$(5)$$

R^2 value was 0.9936. According to Eq. (5), all the effects of factors and the interactions between them were statistically significant ($p < 0.05$) except interactions ACD (p value = 0.407) and ABC (p value = 0.418). The maximum coefficient value was for interaction BD with its + sign between − B (50 mg Tween 80) and − D (mixture of poloxamer). The use of − B with − D leads to a significant increase in particle size and consequently an increase in the volume of entrapped liquid containing the drug. These were discussed previously for the effect of B and D on increasing the size of nano system leading to increasing entrapping efficiency.

The second effective factor was − C (homogenization time 3 min) which leads to an increase in entrapment efficiency as the reduction in the homogenization time increases in particle size and hence the entrapping efficiency.

The third effective factor was + ABD as its ingredients were + A (GMS 250 mg), − B Tween 80 (50 mg), and − D (mixture of poloxamer). Because of the higher level of mono-, di-, and triglycerides, which operate as solubilizers for highly lipophilic medications, it was declared that with increasing the amount of GMS the % EE increases [36, 40]. As a result, the use of a high level of GMS and

a low level of Tween 80 with a poloxamer mixture leads to a significant increase in particle size and consequently increases entrapment efficacy. As a conclusion, the increase in particle size resulted in an increase in entrapment efficiency. Based on these data, the optimum formula with respect to the recorded entrapment efficiency values is F6.

Fig. 1 The release profiles of apixaban from aqueous drug suspension and different solid lipid nanoparticle formulations
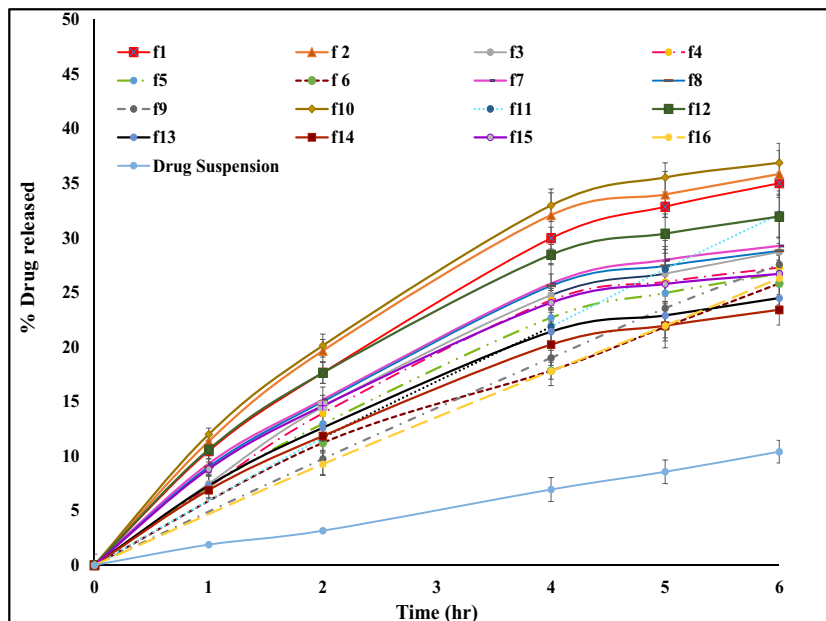
Table V Drug Release Kinetic Parameters of APX-SLnPs Formulations

Formula	Kinetic order	R^2	K	T_{50} (hrs)	%Drug released after 4 h
F1	Higuchi	0.98	14 ± 0.65	12.78 ± 1.2	29.96 ± 2.2
F2	Higuchi	0.96	15 ± 0.9	11.13 ± 1.07	32.07 ± 2
F3	Higuchi	0.993	11.4 ± 0.41	19.18 ± 1.4	24.74 ± 0.6
F4	Higuchi	0.9995	10.8 ± 0.55	21.7 ± 2.3	24.26 ± 0.9
F5	Zero	0.998	5.9 ± 0.13	8.49 ± 0.19	22.8 ± 0.5
F6	Zero	1	4.4 ± 0.13	12.2 ± 1.75	17.8 ± 1.3
F7	Zero	0.9994	6.8 ± 0.22	7.36 ± 0.2	25.8 ± 0.88
F8	Zero	0.999	6.7 ± 0.53	7.5 ± 0.61	25.59 ± 2
F9	Zero	1	4.6 ± 0.1	10.9 ± 0.17	18.99 ± 0.68
F10	Higuchi	0.999	15.2 ± 0.68	10.9 ± 0.96	32.97 ± 1.5
F11	Zero	0.9999	5.5 ± 0.34	9.14 ± 0.49	21.85 ± 1.6
F12	Higuchi	0.992	13.4 ± 0.62	14.1 ± 1.3	28.45 ± 0.93
F13	Higuchi	0.99	9.7 ± 0.43	26.7 ± 2	21.4 ± 0.96
F14	Zero	0.998	5.3 ± 0.32	9.5 ± 0.56	20.2 ± 1.3
F15	Higuchi	0.9985	11 ± 0.22	20.4 ± 0.8	24.05 ± 0.5
F16	Zero	1	4.4 ± 3.9	11.4 ± 0.88	17.8 ± 0.87
Drug suspension	Zero	0.9978	1.7 ± 0.19	29.4 ± 3.5	6.9 ± 1.1

APX-SLnPs, solid lipid nanoparticles loaded with apixaban

In Vitro Apixaban Release

The *in vitro* apixaban release profiles from drug suspension and the developed preparations are shown in Fig. 1. Table V lists the correlation coefficient values (R^2), 50% release time (T50), release rate constants (K) for the release models, and % drug released after 4 h.

$$\%Drug\ released\ after\ 4h = 24.285 + 0.607A - 2.375C$$
$$- 1.077D - 0.650AB - 2.171AC$$
$$+ 1.035AD + 1.615BC + 0.597ABC$$
$$- 0.909ABD - 1.377BCD - 1.334ACD$$
$$(6)$$

R^2 value was 0.9496. According to Eq. (6), all the effects of factors and the interactions among them were statistically significant ($p < 0.05$) except interactions BD (p value = 0.818), ABCD (p value = 0.106), and CD (p value = 0.918) and factors B (p value = 0.242).

The maximum coefficient value was for factor C with its + sign which is homogenization time of 6 min that decreases the % drug released. The high homogenization time gives a higher chance for the solid nano system to be completely formed and stabilized and consequently decreases drug release.

The second effective coefficient value was for interaction + AC which expresses the interaction between + A (GMS 250 mg) and + C (homogenization time (6 min)). Increasing the concentration of the lipid was accompanied by a decrease in the drug release from the SLnPs.

The third effective interaction was − BC which expresses the interaction between + C (homogenization time (6 min)), and − B (Tween 80 (50 mg)). Increasing the amount of surfactant was associated with an increase in the drug release from the SLnPs [41]. So, decreasing surfactant concentration with the increase of homogenization time gives a significant interaction that led to the decreased release. Accordingly, the optimized formula corresponding to decreased drug release is F6. This selection was based on the calculated % drug release after 4 h and 6 h (Table V). After 4 h, F6 and F16 showed similar results. However, F6 showed a smaller % drug release after 6 h (25.8 ± 1.2) compared with F16 (26.28 ± 2.44).

The decreased release rate was preferred with SLnPs as the mechanism of the action of these systems based on their ability to penetrate the biological membrane in intact form and being taken with the lymphatic system. Accordingly, a lower release rate guarantees a higher level of the drug within the vesicles and higher bioavailability.

Fitting the release data to different release kinetic models revealed that the zero-order kinetic model and Higuchi models showed a strong correlation concerning drug release from APX-SLnPs. The formulations F5, F6, F7, F8, F9, F11, F14, and F16 showed a zero-order release profile in which the release of apixaban is concentration-independent providing a constant release rate. This was reported in research work as the ideal behavior for drug delivery systems to guarantee a constant level of the drug at its release site during the delivery time [42]. The regression analysis of the collected data for the other formulations showed the greatest fit to the Higuchi diffusion model. This behavior indicates that a matrix structure may exist which resulted in diffusion-controlled release kinetics. The variability in the release pattern from different SLnPs suggests that the under-researched nano formulation can offer a highly modified release profile. The *in vitro* release of apixaban from drug suspension revealed a limited release rate. This was expected based on the reported lipophilic nature of the drug which made the release process dissolution rate limited. Comparing the release rate from drug suspension with the prepared formulations, the results showed a slower release rate from an aqueous drug suspension. This can be explained based on the ability of SLnPs formulations to improve the release of free apixaban compared to aqueous drug suspensions. Similar release pattern was reported in literatures [43, 44].

Determination of the Optimized Formula

After the application of the response optimizer and according to the previous results, F9 was the optimized formula due to its small particle size (285.7 nm), high entrapment effectiveness (66.8%), and low % release after 4 h (27.5%). This formulation (F9) achieved the preferred size for this nano system keeping an acceptable entrapment efficiency (to be maximized) and drug release rate (to be minimized). The small particle size of F9 was crucial in its selection as the optimized formulation as it was reported that the smaller the particle size, the more efficient will be the nano system [39]. Upon the application of the response optimizer and set entrapment efficiency (to be maximized) and size (to be minimized), the statistical value for desirability achieved for the size and entrapment efficiency was 1. This indicates that the variables in F9 achieved favorable particle size and % entrapment efficiency compared with other formulations. So F9 was chosen as the optimum formula and was subjected to subsequent tests for FTIR, DSC, morphology, and *in vivo* evaluation.

Characterizations of the Optimized APX-SLnPs

Fourier-Transform Infrared Spectroscopy (FTIR)

The spectral pattern of the prepared APX-SLnPs can be confirmed by FT-IR analysis. In Fig. 2, the recorded FTIR spectra are displayed. The spectrum of GMS reveals several

Fig. 2 FTIR spectrum of GMS, poloxamer 188, apixaban, the optimized APX-SLnPs, and its physical mixture
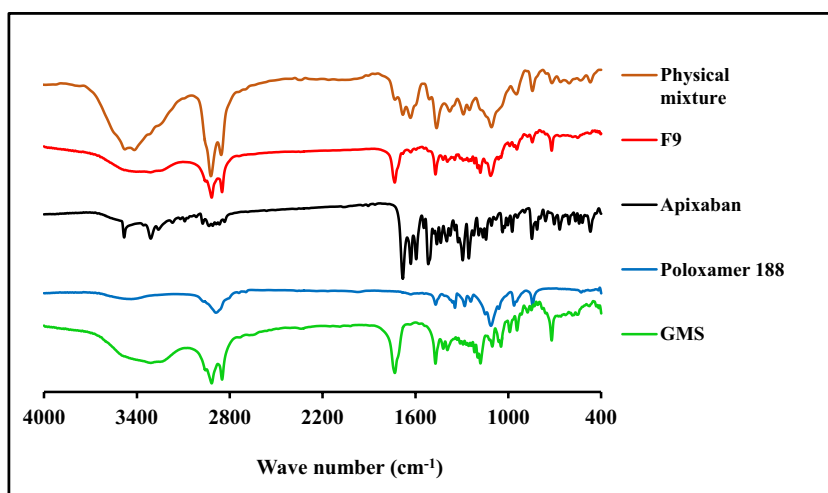
absorption peaks caused by the existence of its main functional groups. The peaks of C–H stretch in the –CH2 groups were observed at 2965 and 2849 cm^{-1} confirming the presence of fatty acid acyl chain. The characteristic absorption peak observed at 1732 cm^{-1} can be accredited to the stretching vibration of C=O group. The stretching vibration of C–O–C in the polar head group was noticed at 1179 cm^{-1}. The broad absorption band which is seen at 3310 cm^{-1} can be attributed to the presence of O–H, the glycerol moiety. Similar spectrum was reported previously for GMS [45]. The FTIR spectrum of pure APX revealed absorption bands at 3482 and 3310 cm^{-1} which are assigned for NH asymmetric and primary NH symmetric vibration. The C–H stretching asymmetric and symmetric of CH3 were noticed at 2974 and 2832 cm^{-1}. The Bands recorded at 1516–1397 cm^{-1},

1255, and 1681 cm^{-1} were assigned for C=C stretching of a benzene ring, N–C and C=O stretching of the amide group respectively. This spectrum was reported previously for apixaban [46]. According to data in the literature, the FTIR spectrum of poloxamer 188 is characterized by main absorption peaks at 3437, 2883, 1344, and 1111 cm^{-1} which can be attributed to OH stretching, aliphatic C–H stretch, in-plane O–H bend, and C–O stretch, respectively. This spectral pattern was reported for poloxamer 188 in several research works [47]. The FTIR spectrum of the optimized formulation showed the main absorption bands of the lipid dominating the spectrum. This was accompanied by the disappearance of the characteristic absorption peaks of apixaban. In contrast, the FTIR spectrum of the prepared physical mixture indicates the presence of the characteristic

Fig. 3 DSC thermograms of apixaban, GMS, poloxamer 188, physical mixture of all solid ingredients at the same ratio in the formula, and the centrifuged form of the optimized SLnPs
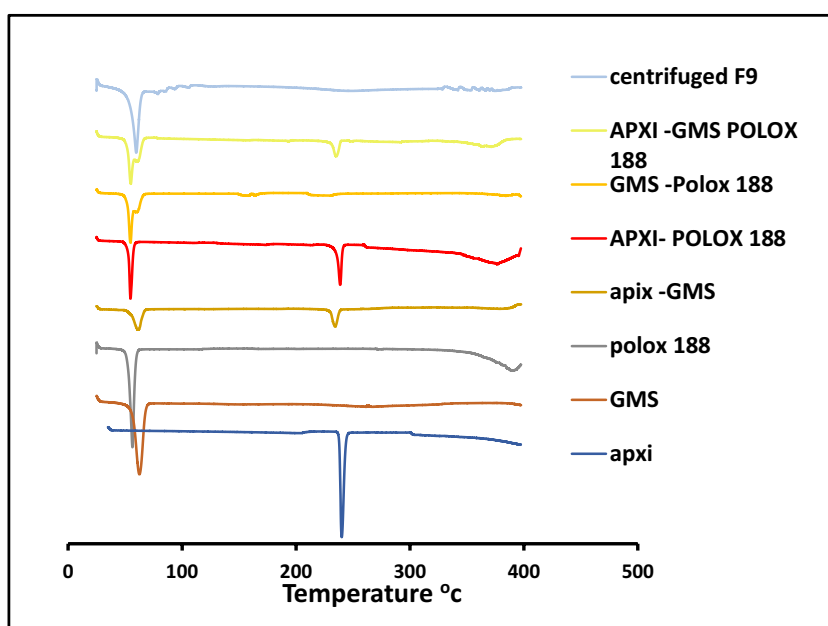
absorption peaks of apixaban. These include that assigned for NH asymmetric and primary NH symmetric vibration in addition to C=O stretching of the amide group. This indicated the possibility of drug encapsulation within the core of the lipid matrix in the optimized formulation. Similar data were reported previously in the literature and were similarly explained [48, 49].

Differential Scanning Calorimetry (DSC)

DSC was utilized to monitor the melting behavior of different crystalline materials in addition to different nano systems. The recorded thermal pattern of pure APX, glycerol mono stearate, poloxamer 188, physical mixtures, and the optimized APX-SLnPs formula (F9) are depicted in Fig. 3. The thermogram of apixaban showed a definite endotherm at Tm 240.16°C. This melting endotherm confirmed the crystalline nature of apixaban and matches with that reported in the literature [50]. The thermogram of GMS revealed the existence of a distinct melting endotherm at 62.59°C which correlates with that stated in different research work [51]. Regarding poloxamer 188, the thermogram showed a sharp endothermic peak at Tm value of 54.89°C [52–54]. The physical mixtures containing these ingredients showed the same endothermic peak indicating no interaction and proving the existence of the drug in its crystalline form. By contrast, the thermogram of the prepared formulations revealed the absence of the main endothermic peak of apixaban. This indicated the solubilization of the drug in the lipids or existence in an amorphous form. This explanation was informed previously by other investigators [55].

Transmission Electron Microscopy

The TEM was employed to assess the morphology and particle size of the optimized nano system. The captured micrograph is presented in Fig. 4. The micrograph revealed the spherical nature of the prepared solid lipid nanoparticles. These particles are in the nanosized range as revealed by the measured particle size values. These values ranged from 64.13 to 70.91 nm. Similar morphological features were reported previously for solid lipid nanoparticles [56]. The difference in nominal values of particle size between TEM and zetasizer can be due to the principles used in particle size determination in both cases. The particle size in TEM depends on the size of particles in the selected field while in zetasizer, it depends on the mobility of the particles in the dispersion. Similar discrepancy between both techniques was stated and explained in previous research works [57, 58].

Evaluation of the Bleeding Effect of Apixaban SLnPs

Bleeding model was employed to probe the *in vivo* efficacy of apixaban-loaded SLnPs. The results of bleeding time measurements are shown in Table VI with the data being presented in the form of a histogram in Fig. 5. The average bleeding time for the naïve (negative control group) was

Table VI The Recorded Bleeding Time Values for Each Experimental Group

Formulations	Negative control	Positive control	Solid lipid nanoparticles
Bleeding time (minutes)	6.67 ± 0.36	10.33 ± 2.86	28.17 ± 2.37

The values represent the mean $\pm$ SEM, $n = 6$

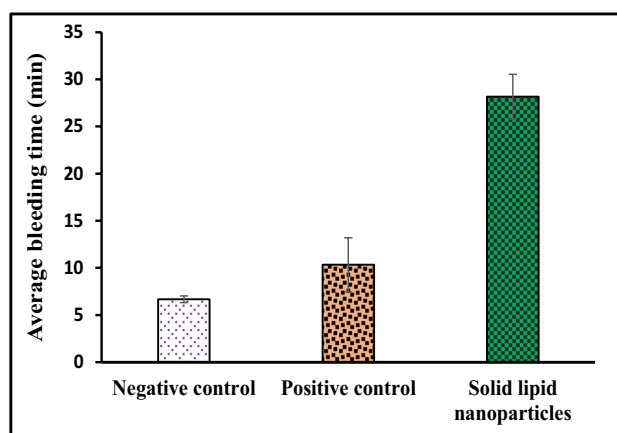**Fig. 4** Transmission electron micrograph of the optimum APX-SLnPs

Fig. 5 The recorded bleeding time for each group presented as mean (mg/dl) $\pm$ standard error

recorded to be 6.67 ± 0.36 min. These data correlated with that reported in the literature [33]. Oral administration of apixaban in the form of aqueous drug suspension (positive control) marginally increased the bleeding time values. Comparing the recorded data collected from negative and positive control groups using Kruskal–Wallis test multiple comparisons employed post-hoc Tukey's test revealed no significant differences between both groups ($p = 0.47$). These results were expected based on the reported poor oral bioavailability of apixaban [23]. Oral administration of apixaban-loaded SLnPs resulted in statistically significant prolongation in bleeding time (28.17 ± 2.37 min) compared with both positive and negative control ($p < 0.001$). This enhancement can be considered as a reflection on the ability of SLnPs to augment the therapeutic effect of drug. The mechanism of this enhancement can be due to the ability of SLnPs to encapsulate high concentration of apixaban; moreover, their small size can facilitate their entrance to the lymphatic system escaping the first-pass metabolism [11]. The efficacy of SLnPs in enhancing the efficacy of drugs with poor bioavailability was reported in the literature [39].

Conclusion

Apixaban-loaded solid lipid nanoparticles were successfully fabricated using homogenization followed by ultrasonication technology. The formulations were optimized utilizing the full factorial design and the optimum APX-SLnPs regarding entrapment efficiency, and controlled particle size was fully characterized and evaluated for its *in vivo* performance. The *in vivo* study using the bleeding time model reflected significant prolongation in bleeding time after oral administration of the optimum APX-SLnPs compared with both negative and positive control. Thus, solid lipid nanoparticles can be employed as an efficient delivery system for enhancing the therapeutic effect of BCS class IV drugs like apixaban.

Declarations

References

1. Ghadi R, Dand N. BCS class IV drugs: highly notorious candidates for formulation development. J Control Release. 2017;28(248):71–95. https://doi.org/10.1016/j.jconrel.2017.01.014.

2. Gunaseelan S, Gunaseelan K, Deshmukh M, Zhang X, Sinko PJ. Surface modifications of nanocarriers for effective intracellular delivery of anti-HIV drugs. Adv drug Deliv Rev. 2010;18;62(4–5):518–31. https://doi.org/10.1016/j.addr.2009.11.021.

3. Sharma P, Garg S. Pure drug and polymer based nanotechnologies for the improved solubility, stability, bioavailability and targeting of anti-HIV drugs. Adv drug Deliv Rev. 2010;18;62(4–5):491–502. https://doi.org/10.1016/j.addr.2009.11.019.

4. Van Eerdenbrugh B, Van den Mooter G, Augustijns P. Top-down production of drug nanocrystals: nanosuspension stabilization, miniaturization and transformation into solid products. Int J Pharm. 2008;19;364(1):64–75. https://doi.org/10.1016/j.ijpharm.2008.07.023.

5. Wu TK, Lin SY, Lin HL, Huang YT. Simultaneous DSC-FTIR microspectroscopy used to screen and detect the co-crystal formation in real time. Bioorganic Med Chem Lett. 2011;15;21(10):3148–51. https://doi.org/10.1016/j.bmcl.2011.03.001.

6. Yadav VB, Yadav AV. Improvement of solubility and dissolution of indomethacin by liquisolid and compaction granulation technique. J Pharm Sci Res. 2009;1;1(3):44.

7. Gursoy RN, Benita S. Self-emulsifying drug delivery systems (SEDDS) for improved oral delivery of lipophilic drugs. Biomed Pharmacother. 2004;1;58(3):173–82. https://doi.org/10.1016/j.biopha.2004.02.001.

8. Rane SS, Anderson BD. What determines drug solubility in lipid vehicles: is it predictable? Adv Drug Deliv Rev. 2008;17;60(6):638–56. https://doi.org/10.1016/j.addr.2007.10.015.

9. Muller RH. Solid lipid nanoparticles (SLNP)-an alternative colloidal carrier system for controlled drug delivery. Eur J Biopharm. 1995;41:62–9.

10 Müller RH, Mäder K, Gohla S. Solid lipid nanoparticles (SLNP) for controlled drug delivery–a review of the state of the art.

Eur J Pharm Biopharm. 2000;3;50(1):161–77. https://doi.org/10.1016/S0939-6411(00)00087-4.

11. Mehnert W, Mäder K. Solid lipid nanoparticles: production, characterization and applications. Adv Drug Deliv Rev. 2012;1(64):83–101. https://doi.org/10.1016/j.addr.2012.09.021.

12. Basha SK, Dhandayuthabani R, Muzammil MS, Kumari VS. Solid lipid nanoparticles for oral drug delivery. Mater Today: Proceedings. 2021;1(36):313–24. https://doi.org/10.1016/j.matpr.2020.04.109.

13. Osanlou R, Emtyazjoo M, Banaei A, Hesarinejad MA, Ashrafi F. Preparation of solid lipid nanoparticles and nanostructured lipid carriers containing zeaxanthin and evaluation of physicochemical properties. Colloids Surf A: Physicochem Eng Aspects. 2022;20(641):128588. https://doi.org/10.1016/j.colsurfa.2022.128588.

14. Yuan H, Chen J, Du YZ, Hu FQ, Zeng S, Zhao HL. Studies on oral absorption of stearic acid SLNP by a novel fluorometric method. Colloids Surf B: Biointerfaces. 2007;1;58(2):157–64. https://doi.org/10.1016/j.colsurfb.2007.03.002.

15. Wang XF, Zhang SL, Zhu LY, Xie SY, Dong Z, Wang Y, Zhou WZ. Enhancement of antibacterial activity of tilmicosin against Staphylococcus aureus by solid lipid nanoparticles in vitro and in vivo. Vet J. 2012;1;191(1):115–20. https://doi.org/10.1016/j.tvjl.2010.11.019.

16. Guo S, Pham K, Li D, Penzak SR, Dong X. Novel in situ self-assembly nanoparticles for formulating a poorly water-soluble drug in oral solid granules, improving stability, palatability, and bioavailability. Int J Nanomedicine. 2016;11:1451. https://doi.org/10.2147/IJN.S100621.

17. Shazly GA, Alshehri S, Ibrahim MA, Tawfeek HM, Razik JA, Hassan YA, Shakeel F. Development of domperidone solid lipid nanoparticles: in vitro and in vivo characterization. AAPS PharmSciTech. 2018;19:1712–9. https://doi.org/10.1208/s12249-018-0987-2.

18. Bhaskar K, Krishna Mohan C, Lingam M, Prabhakar Reddy V, Venkateswarlu V, Madhusudan Rao Y. Development of nitrendipine controlled release formulations based on SLNP and NLC for topical delivery: in vitro and ex vivo characterization. Drug Dev Ind Pharm. 2008;1;34(7):719–25. https://doi.org/10.1080/03639040701842485.

19. Üner M, Yener G. Importance of solid lipid nanoparticles (SLNP) in various administration routes and future perspectives. Int J Nanomedicine. 2007;1;2(3):289–300. https://doi.org/10.2147/IJN.S2.3.289.

20. Harde H, Das M, Jain S. Solid lipid nanoparticles: an oral bioavailability enhancer vehicle. Expert Opin Drug Deliv. 2011;1;8(11):1407–24. https://doi.org/10.1517/17425247.2011.604311.

21. Jain HK, Nikam VK. Formulation development and stability indicating HPLC assay of tablets of apixaban. Int J Pharm Pharm Sci. 2017;2;9(10):24–32. https://doi.org/10.22159/ijpps.2017v9i10.20343.

22. Billett HH, Reyes-Gil M, Szymanski J, Ikemura K, Stahl LR, Lo Y, Rahman S, Gonzalez-Lugo JD, Kushnir M, Barouqa M, Golestaneh L. Anticoagulation in COVID-19: effect of enoxaparin, heparin, and apixaban on mortality. J Thromb Haemost. 2020;120(12):1691–9. https://doi.org/10.1055/s-0040-1720978.

23. Byon W, Garonzik S, Boyd RA, Frost CE. Apixaban: a clinical pharmacokinetic and pharmacodynamic review. Clin Pharmacokinet. 2019;58:1265–79. https://doi.org/10.1007/s40262-019-00775-z.

24. Tarley CR, Silveira G, dos Santos WN, Matos GD, da Silva EG, Bezerra MA, Miró M, Ferreira SL. Chemometric tools in electroanalytical chemistry: methods for optimization based on factorial design and response surface methodology. Microchem J.

2009;1;92(1):58–67. https://doi.org/10.1016/j.microc.2009.02.002.

25. Bingol D, Tekin N, Alkan M. Brilliant Yellow dye adsorption onto sepiolite using a full factorial design. Appl Clay Sci. 2010;1;50(3):315–21. https://doi.org/10.1016/j.clay.2010.08.015.

26. Venkateswarlu V, Manjunath K. Preparation, characterization and in vitro release kinetics of clozapine solid lipid nanoparticles. J Control Release. 2004;24;95(3):627–38. https://doi.org/10.1016/j.jconrel.2004.01.005.

27. Venishetty VK, Chede R, Komuravelli R, Adepu L, Sistla R, Diwan PV. Design and evaluation of polymer coated carvedilol loaded solid lipid nanoparticles to improve the oral bioavailability: a novel strategy to avoid intraduodenal administration. Colloids Surf B Biointerfaces. 2012;15(95):1–9. https://doi.org/10.1016/j.colsurfb.2012.01.001.

28. Baek JS, Cho CW. Surface modification of solid lipid nanoparticles for oral delivery of curcumin: improvement of bioavailability through enhanced cellular uptake, and lymphatic uptake. Eur J Pharm Biopharm. 2017;1(117):132–40. https://doi.org/10.1016/j.ejpb.2017.04.013.

29. Hao YM. Entrapment and release difference resulting from hydrogen bonding interactions in niosome. Int J Pharm. 2011;17;403(1–2):245–53. https://doi.org/10.1016/j.ijpharm.2010.10.027.

30. Sultan AA, El-Gizawy SA, Osman MA, El Maghraby GM. Niosomes for oral delivery of nateglinide: in situ–in vivo correlation. J Liposome Res. 2018;3;28(3):209–17. https://doi.org/10.1080/08982104.2017.1343835.

31. Jenning V, Schäfer-Korting M, Gohla S. Vitamin A-loaded solid lipid nanoparticles for topical use: drug release properties. J Control Release. 2000;15;66(2–3):115–26. https://doi.org/10.1016/S0168-3659(99)00223-0.

32. Eid RK, Essa EA, El Maghraby GM. Essential oils in niosomes for enhanced transdermal delivery of felodipine. Pharm Dev Technol. 2019;7;24(2):157–65. https://doi.org/10.1080/10837450.2018.1441302.

33. Dejana E, Callioni A, Quintana A, de Gaetano G. Bleeding time in laboratory animals. II-A comparison of different assay conditions in rats. Thromb Res. 1979;1;15(1–2):191–7. https://doi.org/10.1016/0049-3848(79)90064-1.

34. Fan C, Song J, White CM. A comparison of the hemostatic effects of notoginseng and yun nan bai yao to placebo control. J Herb Pharmacother. 2005;1;5(2):1–5. https://doi.org/10.1080/J157v05n02_01.

35. Dawaba H. Application of 23 full-factorial design for development and optimization of biocompatible, biodegradable solid lipid nanoparticles containing curcumin. Al-Azhar J Pharm Sci. 2013;48(2):84–101. https://doi.org/10.21608/ajps.2013.7097.

36. Shah M, Pathak K. Development and statistical optimization of solid lipid nanoparticles of simvastatin by using 2 3 full-factorial design. AAPS PharmSciTech. 2010;11:489–96. https://doi.org/10.1208/s12249-010-9414-z.

37. Veni DK, Gupta NV. Development and evaluation of Eudragit coated environmental sensitive solid lipid nanoparticles using central composite design module for enhancement of oral bioavailability of linagliptin. Int J Polym Mater. 2020;2;69(7):407–18. https://doi.org/10.1080/00914037.2019.1570513.

38. Nooli M, Chella N, Kulhari H, Shastri NR, Sistla R. Solid lipid nanoparticles as vesicles for oral delivery of olmesartan medoxomil: formulation, optimization and in vivo evaluation. Drug Dev Ind Pharm. 2017;3;43(4):611–7. https://doi.org/10.1080/03639045.2016.1275666.

39. Wang Y, Pi C, Feng X, Hou Y, Zhao L, Wei Y. The influence of nanoparticle properties on oral bioavailability of drugs. Int J Nanomedicine. 2020;24:6295–310. https://doi.org/10.2147/IJN.S257269.

40. Hao J, Fang X, Zhou Y, Wang J, Guo F, Li F, Peng X. Development and optimization of solid lipid nanoparticle formulation for ophthalmic delivery of chloramphenicol using a Box-Behnken design. Int J Nanomedicine. 2011;6:683–92. https://doi.org/10.2147/IJN.S17386.

41. Ekambaram P, Sathali AA. Formulation and evaluation of solid lipid nanoparticles of ramipril. J Young Pharm. 2011;1;3(3):216–20. https://doi.org/10.4103/0975-1483.83765.

42. Kariminia S, Shamsipur A, Shamsipur M. Analytical characteristics and application of novel chitosan coated magnetic nanoparticles as an efficient drug delivery system for ciprofloxacin. Enhanced drug release kinetics by low-frequency ultrasounds. J Pharm Biomed Analy. 2016;10(129):450–7. https://doi.org/10.1016/j.jpba.2016.07.016.

43. Singh HA, Gupta RA, Gautam GI. Formulation development, characterization, and in vitro-in vivo study of antihyperlipidemic drug rosuvastatin calcium—solid lipid nanoparticles. Asian J Pharm Clin Res. 2018;11(7):436. https://doi.org/10.22159/ajpcr.2018.v11i7.26177.

44. Unnisa A, Chettupalli AK, Al Hagbani T, Khalid M, Jandrajupalli SB, Chandolu S, Hussain T. Development of dapagliflozin solid lipid nanoparticles as a novel carrier for oral delivery: statistical design, optimization, in-vitro and in-vivo characterization, and evaluation. Pharmaceuticals. 2022;2;15(5):568. https://doi.org/10.3390/ph15050568.

45. Patel MN, Lakkadwala S, Majrad MS, Injeti ER, Gollmer SM, Shah ZA, Boddu SH, Nesamony J. Characterization and evaluation of 5-fluorouracil-loaded solid lipid nanoparticles prepared via a temperature-modulated solidification technique. AAPS PharmSciTech. 2014;15:1498–508. https://doi.org/10.1208/s12249-014-0168-x.

46. Abdulbaqi MR, Rajab NA. Preparation, characterization and ex vivo permeability study of transdermal apixaban O/W nanoemulsion based gel. Iraqi J Pharm Sci. 2020;30;29(2):214–22. https://doi.org/10.31351/vol29iss2pp214-222.

47. Garala K, Joshi P, Shah M, Ramkishan A, Patel J. Formulation and evaluation of periodontal in situ gel. Int J Pharm Investig. 2013;3(1):29. https://doi.org/10.4103/2230-973X.108961.

48. Ansari MJ, Anwer MK, Jamil S, Al-Shdefat R, Ali BE, Ahmad MM, Ansari MN. Enhanced oral bioavailability of insulin-loaded solid lipid nanoparticles: pharmacokinetic bioavailability of insulin-loaded solid lipid nanoparticles in diabetic rats. Drug Deliv. 2016;23;23(6):1972–9. https://doi.org/10.3109/10717544.2015.1039666.

49. Kumar R, Singh A, Garg N. Acoustic cavitation-assisted formulation of solid lipid nanoparticles using different stabilizers. Acs Omega. 2019;7;4(8):13360–70. https://doi.org/10.1021/acsomega.9b01532.

50. Asati Amit V, Salunkhe Kishor S, Chavan MJ. Solubility enhancement of BCS classified IV drug-apixaban by preparation and evaluation of mesoporous nanomatrix. Int J Pharm Sci Res. 2020;11:880–90.

51. Patel MH, Mundada VP, Sawant KK. Fabrication of solid lipid nanoparticles of lurasidone HCl for oral delivery: optimization, in vitro characterization, cell line studies and in vivo efficacy in schizophrenia. Drug Dev Ind Pharm. 2019;3;45(8):1242–57. https://doi.org/10.1080/03639045.2019.1593434.

52. Passerini N, Albertini B, González-Rodríguez ML, Cavallari C, Rodriguez L. Preparation and characterisation of ibuprofen–poloxamer 188 granules obtained by melt granulation. Eur J Pharm Sci. 2002;1;15(1):71–8. https://doi.org/10.1016/S0928-0987(01)00210-X.

53. Shah AV, Serajuddin AT. Development of solid self-emulsifying drug delivery system (SEDDS) I: use of poloxamer 188 as both solidifying and emulsifying agent for lipids. Pharm Res. 2012;29:2817–32. https://doi.org/10.1007/s11095-012-0704-x.

54. Sruti J, Patra CN, Swain SK, Beg S, Palatasingh HR, Dinda SC, Rao MB. Improvement in dissolution rate of cefuroxime axetil by using poloxamer 188 and Neusilin US2. Indian J Pharm Sci. 2013;75(1):67. https://doi.org/10.4103/0250-474x.113551.

55. Garg A, Bhalala K, Tomar DS. In-situ single pass intestinal permeability and pharmacokinetic study of developed Lumefantrine loaded solid lipid nanoparticles. Int J Pharm. 2017;10;516(1–2):120–30. https://doi.org/10.1016/j.ijpharm.2016.10.064.

56. Singh M, Mishra R, Dubey S, Roy P, Singh RP. Surface grafted core-shell chitosan-modified solid lipid nanoparticles: characterization and application in hydrophobic drug delivery. In2019 IEEE 14th International Conference on Nano/Micro Engineered and Molecular Systems (NEMS) 2019;11;529–533. https://doi.org/10.1109/NEMS.2019.8915648.

57. Eid RK, Arafa MF, Ashour DS, Essa EA, El-Wakil ES, Younis SS, El Maghraby GM. Surfactant vesicles for enhanced antitoxoplasmic effect of norfloxacin: in vitro and in vivo evaluations. Int J Pharm. 2023;10(638):122912. https://doi.org/10.1016/j.ijpharm.2023.122912.

58. Sultan AA, Saad GA, El Maghraby GM. Permeation enhancers loaded bilosomes for improved intestinal absorption and cytotoxic activity of doxorubicin. Int J Pharm. 2023;2023(630):122427. https://doi.org/10.1016/j.ijpharm.2022.122427.